PETROPHYSICS, VOL. 61, NO. 2 (APRIL 2020); PAGES 189–205; 10 FIGURES; 2 TABLES. DOI: 10.30632/PJV61N2-2020a5

Workflow for Upscaling Wettability From the Nanoscale to Core Scale[1]

Maja Rücker[2,4], Willem-Bart Bartels[3,4], Tom Bultreys[2,5,7], Marijn Boone[8], Kamaljit Singh[6,7], Gaetano Garfi[7], Alessio Scanziani[7], Catherine Spurin[7], Sherifat Yesufu-Rufai[2], Samuel Krevor[7], Martin J. Blunt[7], Ove Wilson[4], Hassan Mahani[4], Veerle Cnudde[3,5], Paul F. Luckham[2], Apostolos Georgiadis[2,4] and Steffen Berg[2,3,7]

ABSTRACT

Wettability is a key factor influencing multiphase flow in porous media. In addition to the average contact angle, the spatial distribution of contact angles throughout the porous medium is important, as it directly controls the connectivity of wetting and nonwetting phases. The controlling factors may not only relate to the surface chemistry of minerals but also to their texture, which implies that a length-scale range from nanometers to centimeters has to be considered. So far, an integrated workflow addressing wettability consistently through the different scales does not exist. In this study, we demonstrate that such a workflow is possible by combining microcomputed tomography (μCT) imaging with atomic-force microscopy (AFM). We find that in a carbonate rock, consisting of 99.9% calcite with a dual-porosity structure, wettability is ultimately controlled by the surface texture of the mineral. Roughness and texture variation within the rock control the capillary pressure required for initializing proper crude oil-rock contacts that allow aging and subsequent wettability alteration. AFM enables us to characterize such surface-fluid interactions and to investigate the surface texture. In this study, we use AFM to image nanoscale fluid-configurations in 3D at connate water saturation and compare the fluid configuration with simulations on the rock surface, assuming different capillary pressures.

INTRODUCTION

Wettability is the preference of a solid to be in contact with one fluid over another fluid. In petroleum applications, rock represents the solid phase, crude oil the first fluid phase and brine, which may be either present in the reservoir (formation water) or injected for oil recovery, the second fluid phase. A rock surface is called water-wet when the water tends to cover it and is called oil-wet when it prefers to be in contact with the oil phase. Furthermore, wettability may vary from location to location with a mixture of water-wet and oil-wet regions. In this case, the rock is called mixed-wet (Brown and Fatt, 1956; Salathiel, 1973; Anderson, 1986; Abdallah et al., 2007; Donaldson and Alam, 2008a).

Wettability by itself is not a property used as a direct input parameter for reservoir models. Yet, it is known to significantly impact input values, such as relative permeability-saturation and capillary pressure-saturation functions (Anderson, 1987a, b; Donaldson and Alam, 2008b). So far, these relationships can only be determined with core-scale experiments. To predict these parameters for a specific reservoir, a better understanding of the principles behind wettability is crucial.

In a reservoir, the wettability depends on various properties which act at different length scales. An overview of the different properties over increasing length scales is shown in Fig. 1. Brine and crude oil composition, surface chemistry and the *P-T* conditions affect molecular interactions, which can be assessed, for instance, through adhesion-force measurements obtained with atomic-force microscopy (AFM) (Hassenkam et al., 2009; Matthiesen et al., 2014; Hassenkam et al., 2015).

Manuscript received by the Editor December 16, 2019; revised manuscript received February 11, 2020; manuscript accepted February 17, 2020.
[1]Originally presented at the International Symposium of the Society of Core Analysts, Pau, France, August 26–29, 2019, Paper SCA2019-007.
[2]Department of Chemical Engineering, Imperial College London, South Kensington Campus, SW7 2AZ London, UK; m.rucker15@imperial.ac.uk; tom.bultreys@ugent.be; s.yesufu17@imperial.ac.uk; p.luckham01@imperial.ac.uk; a.georgiadis@shell.com; steffen.berg@shell.com
[3]Earth Sciences Department, Utrecht University, Princetonlaan 8A, 3508 TC Utrecht, NL; willembart.work@gmail.com; veerle.cnudde@ugent.be
[4]Shell Global Solutions International B.V., Grasweg 31, 1031 HW Amsterdam, NL; o.wilson@shell.com; h.mahani@shell.com
[5]UGCT- PProGRess, Ghent University, Krijgslaan 281 - Building S8, 9000 Ghent, BE
[6]Institute of GeoEnergy Engineering, Heriot-Watt University, EH14 4AS Edinburgh, UK; k.singh@hw.ac.uk
[7]Department of Earth Science and Engineering, Imperial College London, South Kensington Campus, SW7 2AZ London, UK; g.garfi17@imperial.ac.uk; alessio.scanziani16@imperial.ac.uk; catherine.spurin13@imperial.ac.uk; s.krevor@imperial.ac.uk; m.blunt@imperial.ac.uk
[8]Tescan XRE, Bollenbergen 2B bus 1, 9052 Ghent, BE; marijn.boone@tescan.com

At the subpore-scale, roughness, which may facilitate the formation of thin water or oil films, becomes an additional factor. On this length scale, the contact angle forming along three-phase contact lines may be measured (Morrow, 1975). At the larger pore- and pore-network-scale (µm to mm), the confined space within a porous medium is taken into account. Mineralogy and mineral distribution, as well as the saturation history, need to be considered. On this length scale, wettability can be characterized through contact-angle distributions (Andrew et al., 2014), fluid distributions (Herring et al., 2013), by defining local capillary pressure (Armstrong et al., 2012; Herring et al., 2016) and small-scale relative permeability (Berg et al., 2016; Bultreys et al., 2018).

To predict wettability at the core scale the contribution of each consecutive scale to the overall wettability of the system needs to be considered.

Wettability at the Molecular Scale

Most minerals of reservoir rock are originally strongly water-wet (Benner et al., 1938; Anderson, 1986; Hassenkam et al., 2009). However, the adsorption of surface-active components or the precipitation of asphaltenes present in the crude oil may alter the wettability towards more oil-wet (Anderson, 1986; Akhlaq et al., 1996; Buckley, 2001; Kumar et al., 2005; Fernø et al., 2010). Correspondingly, crude oils are usually classified by assessing their acid (TAN) and base (TBN) numbers as well as saturate, aromatics, resins and asphaltene (SARA) fractions, which indicate the stability of asphaltenes within the crude (Fan et al., 2002; White et al., 2018).

In addition to the chemistry of the crude oil and the rock, the brine composition may also impact the wettability. Along a mineral surface, the balance between electrostatic forces and van der Waals forces leads to a double layer of counter ions of the brine phase in correspondence with Derjaguin-Landau-Verwey-Overbeek (Derjaguin and Landau, 1941; Verwey et al., 1948) (DLVO theory), which impacts the repulsive/attractive forces of approaching oil molecules especially in low-salinity systems (Hirasaki, 1991; Israelachvili, 2011; Purswani et al., 2017).

Various studies addressed the impact of these different components (Buckley et al., 1997; Drummond and Israelachvili, 2004; Purswani et al., 2017; Bartels et al., 2019a). In this work, we keep these values constant by focusing on specific crude oil/rock/brine systems to assess the impact of various parameters controlling wettability at larger length scales.

Wettability at the Subpore Scale

At the subpore scale the measure of wettability is the contact angle, which can be obtained by imaging a droplet on a surface e.g. with a contact-angle goniometer (Leach et al., 1962; McCaffery and Mungan, 1970; Treiber and Owens, 1972; Neumann and Good, 1979; Hjelmeland and Larrondo, 1986; Mennella et al., 1995; Giro et al., 2017; Deng et al., 2018). However, subresolution features are known to impact the observed response. Surface roughness may lead to pinning and therewith to a range of possible equilibrium contact angles (Wenzel, 1936; Morrow, 1975; Broseta et

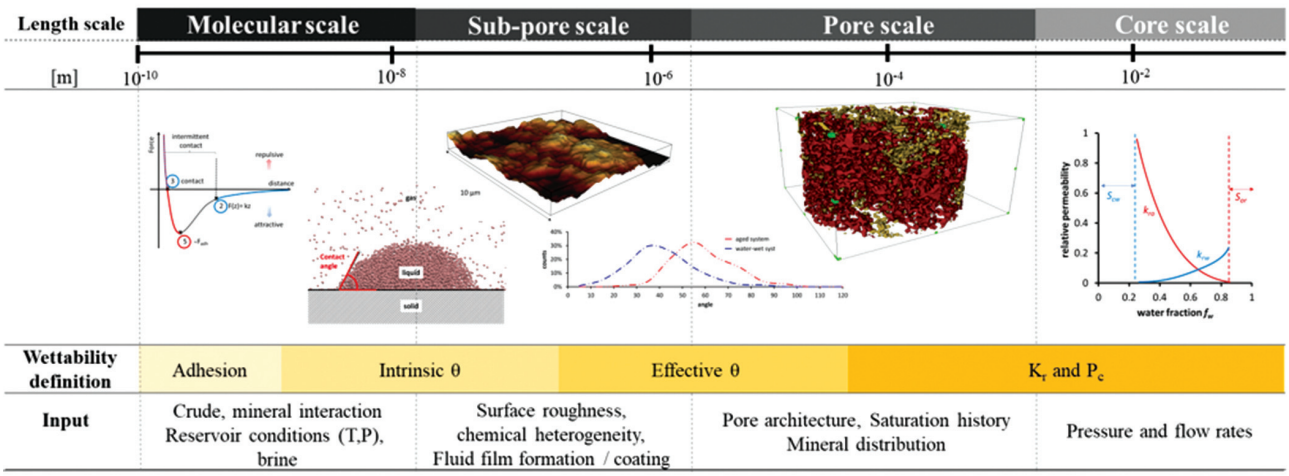

Fig. 1—Wettability depends on various properties acting at different length scales, such as brine- and crude-oil composition, reservoir pressure and temperature (*P*-*T*) conditions, surface chemistry associated with mineralogy at the molecular scale, surface structure and fluid-film formation at the subpore scale as well as saturation history and mineral distribution at the pore scale. They all influence wettability, and thereby the pore dynamics during two-phase flow and the relative permeability (Rücker, 2018).

al., 2012). This effect even occurs on surfaces considered atomically flat (Fogden, 2011; Broseta et al., 2012). Correspondingly, any contact angle measured represents an effective contact angle θ_e. The intrinsic contact angle θ_i, which is solely related to the molecular interactions, is only a theoretical descriptor obtained, e.g., through molecular models assuming a perfectly smooth surface with the fluid phases in equilibrium (Morrow, 1975; Santiso et al., 2013).

Dynamic contact-angle measurements allow the assessment of roughness through an advancing contact angle θ_a and receding contact angle θ_r, which represent the upper and lower boundary of possible contact angles for the studied surface. The detected contact-angle hysteresis depends on the intrinsic contact angle, the surface roughness and velocity of the moving contact line (Morrow, 1975).

Furthermore, natural grooves on a rough surface lead to entrapment of the wetting phase (Kovscek et al., 1993; Herminghaus, 2000; Quéré, 2008). This can have large effects on the wettability alteration process. During drainage, in most cases, the aqueous phase is wetting and forms water films and layers within such grooves. These water films and layers prevent the intimate contact between the oil and the solid and, therewith, wettability alteration in these regions. Correspondingly, such water films may lead to mixed wettability patterns along the surface (Salathiel, 1973; Buckley et al., 1996; Buckley, 2001; Rücker et al., 2019a).

Wettability at the Pore Scale

So far, most 3D studies on mixed-wet and oil-wet rock systems have focused on wettability characterization. Andrew et al. (2014) introduced in-situ measurements of contact angles in rock and Scanziani et al. (2017) and AlRatrout et al. (2017) automated the process. Contact-angle distributions are sensitive to image resolution and may vary in case of nonequilibrium conditions (Andrew et al., 2014). However, they provide an indication of the wettability and wettability changes of the system. Alhammadi et al. (2017) showed a shift of the contact-angle distribution when the wettability of the rock is altered by aging. Yet, these contact angles are not sufficient for prediction of larger-scale relative permeabilities. The obtained distribution does not necessarily cover the advancing contact angle θ_a, which is used as input for most multiphase-flow models in porous media, nor its spatial distribution in case of a mixed-wet rock (Bultreys et al., 2018).

Another way to characterize wettability is through fluid distribution. In oil-wet and mixed-wet systems, the oil clusters appear sheet-like and flat compared to the more spherical geometry in water-wet systems (Al-Raoush, 2009; Iglauer et al., 2012). Singh et al. (2016) observed oil layer formation on the rock surface and between two water interfaces, which provides a conductive flow path for the oil phase in mixed-wet systems. Lin et al. (2019a) observed the formation of minimal fluid-fluid interfaces with a mean curvature of approximately zero with principal curvatures of opposite sign. The fluid-phase distribution or geometry may be fully characterized through morphological descriptors known as the four Minkowski functionals: volume, surface area, integrated mean curvature and Euler characteristic (Joekar-Niasar et al., 2008; Lehmann et al., 2008; Vogel et al., 2010; Herring et al., 2013; Schlüter et al., 2016; Armstrong et al., 2018).

Recent work focuses on linking the pore-scale wettability parameter to core-scale properties, such as capillary pressure-saturation and relative permeability-saturation relationships (Armstrong et al., 2012; Berg et al., 2016; Herring et al., 2017; Lin et al., 2018; Zou et al., 2018).

Wettability at the Core Scale

In conventional special core analysis (SCAL) experiments, the capillary pressure-saturation relationship is used to assess the wettability of a system. This relationship can be obtained by combining the Amott spontaneous imbibition test, in which the cumulative production of the displaced phase versus time is recorded as well as waterfloods to obtain the forced part of the capillary pressure. Various indices, with the Amott and USBM index being the most common, have been introduced to derive wettability from the capillary pressure-saturation relationship (Amott, 1959; Donaldson et al., 1969). However, the results of such experiments are difficult to interpret as other factors besides wettability may impact the results. These factors include, for instance, viscosity, interfacial tension and flow dynamics (Mattax and Kyte, 1962; Ma et al., 1997; Schmid and Geiger, 2013). An alternative is the wettability characterization by rescaling the Leverett J function to provide an average contact angle (Leverett, 1941; Zou and Armstrong, 2019). Yet, this method is not able to account for mixed wettability.

The wettability of a system can also be inferred from the relative permeability-saturation functions using the endpoint water relative permeability, oil-layer drainage and shape of the water relative permeability: An endpoint permeability $k_{rw}^{max} < 0.3$ indicates a water-wet system, $0.3 < k_{rw}^{max} < 0.6$ a mixed wet and $k_{rw}^{max} > 0.6$ an oil-wet system. Oil-layer drainage can be assessed from k_{ro} near to the endpoint: If $k_{ro} < 0.05$, while the saturation is still decreasing, oil is moving through a continuous oil layer, which is indicative of a mixed- or

oil-wet system. If the shape of k_{rw} shows a sharp rise with a crossover saturation $S_w^{cross} < 0.5$, the system is often oil-wet. A low $k_{rw} < 0.2$ for $S_w = S_{wi} + 0.2$ is indicative of a water-wet system (Blunt, 2017).

To predict the described core-scale output using computational models, this behavior needs to be linked to the smaller-scale wettability responses. In this work, we combine the results of various experiments across length scales using similar systems to describe this relationship.

METHODOLOGY

In this work, we compiled the results of previous studies addressing wettability in similar systems (Bartels et al., 2017a, 2017b; Bartels, 2018; Rücker, 2018; Rücker et al., 2019a) and complemented the results with additional measurements to obtain wettability descriptions across all length scales.

Sample Selection

Crude Oil. The crude oils were chosen based on their high wettability alteration potential. The corresponding total acid number (TAN) and total base number (TBN) as well as the saturates, aromatics, resins, asphaltene (SARA) analysis are listed in Table 1. The crude oils are rich on surface-active components and asphaltenes, which represent the components that are expected to change the wettability of the rock.

Crude Oil B was doped with 20% iododecane, to enhance the contrast to the brine phase for μCT imaging. In all experiments with Crude Oil A, the brine phase was doped with potassium iodide. In one experiment, n-decane was used as a model oil.

Brine. The brine composition used in the current studies is listed in Table 2. The formation water (FW) recipe, typical for a carbonate reservoir, was taken from Mahani et al. (2015). For the first study with a doped brine a 17 wt% KI-brine was chosen. Based on the ionic strength this corresponds to 70,400 ppm NaCl and therefore is considered a high-salinity solution (HS). For the other experiment a 9 wt% KI-brine (S) was chosen to obtain a better contrast between the two fluid phases. This brine has the same ionic strength as a 37,300 ppm NaCl brine solution, which is above the threshold for the low-salinity effect (Mahani et al., 2017). Any impact on wettability is therefore considered minor.

Rock. The rock samples from the Ketton quarry (herein called "Ketto rock"), Rutland, England, are middle Jurassic oolithic carbonate rocks consisting of round grains (ooids and peloids) ranging from 100 μm to 1 mm in size. Oolites are marine sediments, which form during evaporation. Dissolved carbonate precipitates along nuclei floating in the seawater, which leads to concentric growth and the round shape of the grains. Once the particles become too heavy, they accumulate at the seafloor, where they become cemented (Flügel, 2004). The geological history of the formation leads to a homogeneous and simple structure of the rock, which makes the rock highly suitable for microcomputed tomography (μCT) flow experiments (Andrew et al., 2015; Singh et al., 2017, Rücker et al., 2019a).

The rock has a porosity of $\phi = 23\%$ with a bimodal pore-size distribution and permeability of 3 to 6 D. It consists predominantly of calcite (99.1%) with minor quartz (0.9%) components (Andrew, 2015).

Core-Scale Wettability Assessment

At the core scale, wettability can be derived from relative permeability-saturation and capillary pressure-saturation functions. These can be obtained through special core analysis (SCAL) experiments, such as steady-state corefloods or Amott spontaneous imbibition tests.

Table 1—TAN, TBN, SARA Fractions, Viscosity and Density of the Crude Oils Used

	TAN (mg KOH/g)	TBN (mg/kg)	Saturates (wt%)	Aromatics (wt%)	Resins (wt%)	Asphaltenes (wt%)	Viscosity 20°C (mPa s)	Density 20°C (g/cm^3)
Crude A	0.07	83.9	58.45	44.00	4.36	0.28	4.87	0.83
Crude B	0.38	2.86	52.08	39.06	7.96	0.91	17.03	0.85

Table 2—Composition of Formation Water (FW) and a High-Salinity Brine (HS) Used

ION (mg/L)	Na^+	K^+	Mg^{2+}	Ca^{2+}	Cl	SO_4^{2-}	HCO^{3-}	I^-	Ionic Strength (mol/L)	pH
FW	49898	0	3,248	14,501	111,812	234	162	0	3.659	6.9
HS (doped)	0	47,106	0	0	0	0	0	152,894	1.205	--
S (doped)	0	21,198	0	0	0	0	0	68,802	0.542	--

Steady-State Coreflood Experiment. Experiments to determine relative permeability were performed in a custom-built X-ray saturation measurement apparatus at Shell (Kokkedee et al., 1996; Berg et al., 2008; Berg et al., 2016) following the steady-state method (Dake, 1983; McPhee et al., 2015).

The Ketton sample (SCAL-plug: diameter d = 2.5 cm and length L = 5 cm) was first saturated with HS-brine and then mounted inside an X-ray transparent core holder and placed in the flow apparatus for a steady-state relative permeability measurement. Afterwards, the sample was desaturated with Crude Oil A by flooding at 1 mL/min until no further change in saturation was detected. The sample was then aged at 3 MPa and 70°C for 1 week. The measurements were conducted at a constant flow rate, where the fractional flow f_w was systematically changed from 100% crude oil to 100% HS-brine in 10 steps (f_{w1} = 0.01; f_{w2} = 0.05; f_{w3} = 0.1; f_{w4} = 0.3; f_{w5} = 0.5; f_{w6} = 0.7; f_{w7} = 0.9; f_{w8} = 0.95; f_{w1} = 0.99; f_{w10} = 1). At each step, saturation (and spatial profile along the core) and phase pressures were recorded after steady-state was reached. The SCAL data (pressure drop over the core and saturation profiles at each fractional flow step) were matched numerically using Shell's in-house simulator (MoReS) to estimate the relative permeability as a function of saturation.

Amott Spontaneous Imbibition Tests. In an Amott spontaneous imbibition test an oil-saturated rock sample is placed into a vessel containing FW-brine. In water-wet and mixed-wet samples the water starts to spontaneously imbibe into the rock sample replacing the oil, which then gets produced, collected and monitored over time. The production rate and the cumulative production are used as a measure for wettability (Amott, 1959).

Bartels et al. (2017a) conducted an Amott spontaneous imbibition test on a SCAL plug sample and a miniplug sample commonly used for μCT studies (miniplug: diameter d = 4 mm and length L = 20 mm).

Both samples were cleaned, saturated with FW-brine and then desaturated with Crude Oil B. The SCAL plug was desaturated by centrifugation (URC-628, 129 Coretest Systems Inc., used at 3,500 RPM) for 24 hours while the temperature was kept constant at 40°C. The miniplug was desaturated by flooding 0.5 mL/min and then placed into an oven at 40°C for 24 h.

Consecutively, the samples were placed into Amott vessels. The production of the SCAL plug was monitored with HECTOR, a high-energy μCT scanner at the Centre for X-ray Tomography (UGCT) in Ghent, Belgium (Masschaele et al., 2013), and the production of the miniplug with the Environmental MicroCT scanner (EMCT) also at UGCT (Bultreys et al., 2016). The scans were reconstructed using dedicated reconstruction tools in the Acquila software package from Tescan XRE. Visualization and additional post-processing of the data were performed with Avizo 9.2.0 (Thermo Fischer Scientific). The detailed experimental procedures can be found in Bartels et al. (2017a).

Pore-Scale Wettability Assessment

Lin et al. (2019b) stated that sample initialization, especially flooding as opposed to centrifugation, may have a significant impact on the outcome. For this reason, both initialization protocols (centrifugation and flooding) were assessed at the pore scale.

Unsteady-State Waterflood Experiments Initialized by Flooding. The unsteady-state waterflood experiment was obtained from Rücker et al. (2019b). The miniplug samples were first saturated with HS-brine and then desaturated with Crude A by flooding 0.5 mL/min using the flow cell described in Armstrong et al. (2014). The samples were aged at 3MPa and 70°C for one week. The waterflood was performed at a flow rate of 0.03 mL/min. During the experiment the fluid distributions within the sample were monitored using fast μCT facility at the TOMCAT-SLS beamline at the Paul Scherrer Institute, PSI, in Switzerland, while the HS-brine was injected into the sample.

The images were reconstructed using the Paganin method (Paganin et al., 2002) and processed and segmented with Avizo 9.0. The wettability of the system was assessed visually and by contact-angle measurements following the workflow described in Andrew et al. (2014) using the filtered grayscale image of the final time step measured during this flooding sequence.

Unsteady-State Waterflood Experiments Initialized by Centrifugation. The unsteady-state waterflood performed on a centrifuged sample was prepared following the protocols from Lin et al. (2019b). Eight subsamples with a diameter of 6 mm and length L = 20 mm were predrilled in a SCAL plug with a diameter of 3.8 cm and length L = 4 cm. Subsequently, the plug was saturated with S-brine, desaturated in a centrifuge with Crude A (URC-628, 129 Coretest Systems Inc., used at 3,500 RPM for 24 h) and then stored at elevated pressure of 3 MPa and temperature of 70°C for 4 weeks. Afterwards, the smaller sample was gently chopped off the SCAL plug with tweezers and fitted into the Viton sleeve while being kept in the crude oil and placed into a core holder described in Singh et al. (2016). Consecutively, a waterflood experiment was performed by injecting S-brine at a flow rate of 0.03 mL/min for 2 h. μCT

scans with a voxel size of 6.1 µm were taken for the full sample and two smaller (988×1,014×997) subsamples with a voxel size of 2 µm prior to and after the experiment using a Xradia µCT-scanner (Zeiss).

The images were reconstructed using the proprietary software provided by Zeiss, filtered with a nonlocal means filter and segmented with the trainable WEKA segmentation tool (Arganda-Carreras et al., 2017) provided by Fiji (Schindelin et al., 2012). The contact-angle distribution was measured manually using the filtered image obtained after the waterflood following the procedure described in Andrew et al. (2014).

Topographical Measurements With AFM

At the subpore scale the impact of the surface structure of a rock was assessed with atomic-force microscopy (AFM). As illustrated in Fig. 2., AFM images the topography of a surface mechanically. The surface of the rock is raster scanned by an atomically sharp tip attached to the end of a cantilever.

Close to the surface, intermolecular forces acting on the tip lead to a bending of the cantilever, which is monitored by a laser. For the measurements presented, special attention was given to the location at which the rock was scanned, to avoid spots affected by drilling or breakage. The rock surface was scanned with a silicon tip (PPP-NCHAuD from NANOSENSORS™) along a 10 µm × 10 µm area (128×128 pixels) using the Quantitative Imaging mode (QI™-mode). In this mode at each pixel a full force-distance profile is obtained (i.e., the force between the AFM tip and the surface is monitored as the tip approaches the surface). The rock sample was first saturated with S-brine and then desaturated with n-decane by flooding (500 µL/min) to mimic the distribution of fluid films and layers at the end of drainage. In addition, test experiments were performed on calcite minerals cleaved in oil and cleaved in FW-brine and then submerged in oil.

The image was analyzed with JPKSPM data processing software (JPK instruments) and then transformed into a 3D image using MATLAB (R2018b). These 3D images were then further processed with Geodict 2015 (Math2Market). A morphological drainage simulation assuming a water-wet contact angle of 30° (Hilpert and Miller, 2001) was applied. Avizo 9.0(a) was used for visualization.

RESULTS AND DISCUSSION

Wettability at the Core Scale

Figure 3 shows the core-scale responses obtained from the core-scale steady-state flooding experiment and the Amott spontaneous imbibition test. The results show a difference in wettability depending on the sample initialization.

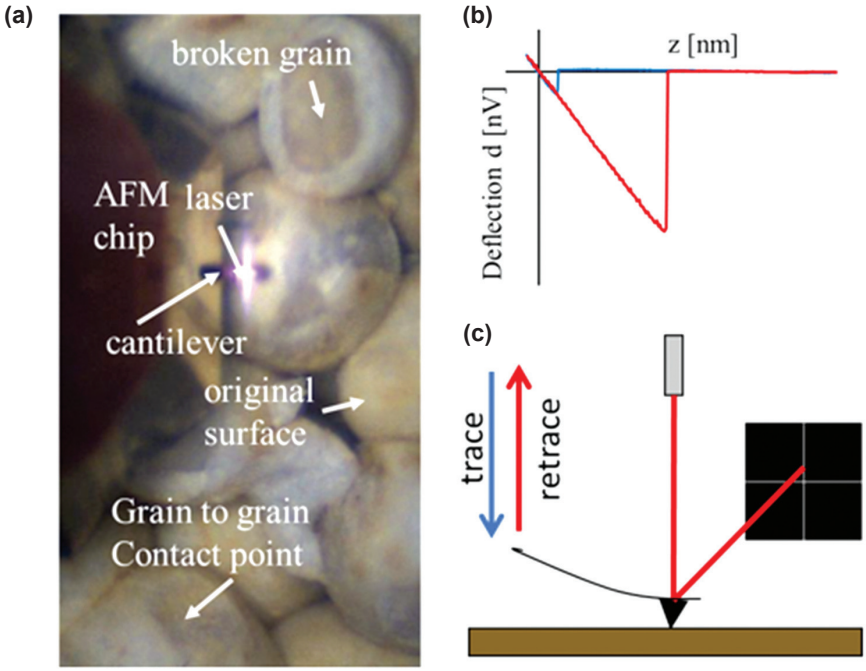

Fig. 2—AFM was used to image the surface of the original rock surface within a pore (a) using QI™-mode, which creates a force distance curve at each pixel (b) by monitoring the deflection of a cantilever with an atomic sharp tip as it approaches and disengages from the surface (c) (Rücker, 2018; Rücker et al., 2020).

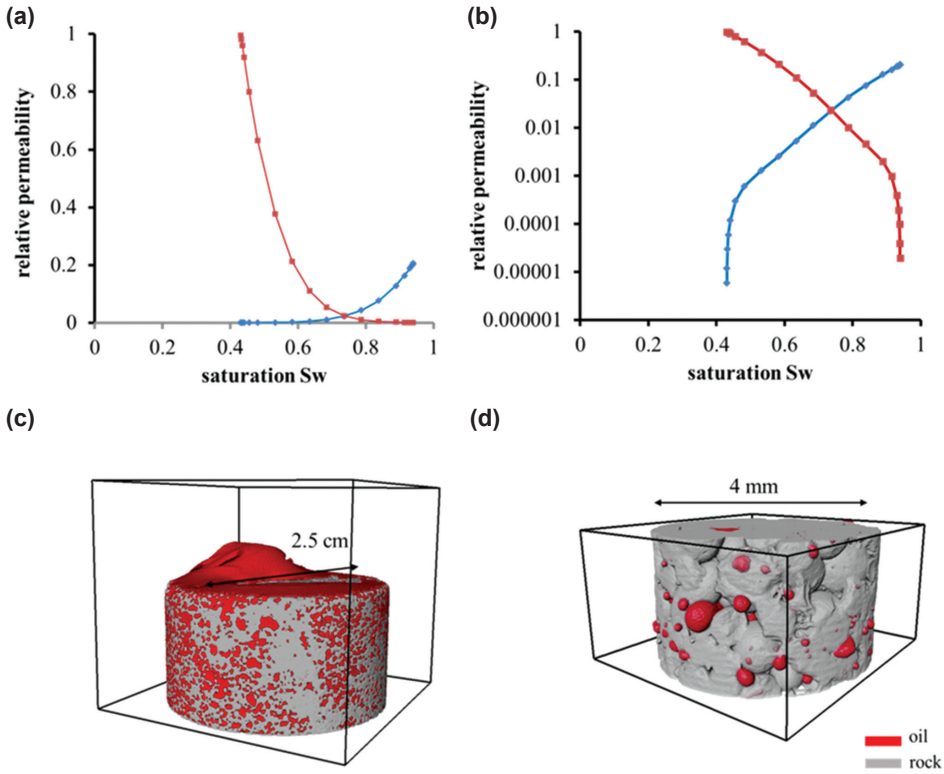

Fig. 3—The core-scale steady-state SCAL experiment initialized by flooding shows a relative permeability, here displayed on an arithmetic (a) and semilogarithmic scale (b), which is typical for a mixed-wet system leaning towards the water-wet side (Rücker, 2018). As the oil droplets (red) emerging from the rock illustrate, the Amott spontaneous imbibition tests show an oil-wet behavior for the sample initialized by centrifugation (c, imaged using HECTOR) and water-wet behavior for the sample initialized by flooding (d, imaged using EMCT) (Bartels et al., 2017a; Rücker, 2018).

The samples prepared by flooding appear mixed-wet to water-wet. Following the guidelines to assess wettability from relative permeabilities by Blunt (2017), the steady-state experiment initialized by flooding appears with a water permeability endpoint of $k_{rw}^{max} = 0.2$ at the upper limit for a water-wet system, but would not yet be considered mixed-wet. However, with a very low residual oil saturation of $S_{res,o} = 0.06$ and a low water relative permeability at low water saturations ($< S_{wi+0.2}$) of $k_{rw}(S_{wi} + 0.2) = 0.03$, this system fulfils two of three criteria proposed to identify a mixed-wet system and correspondingly, is considered mixed-wet leaning to the water-wet side.

The Amott spontaneous imbibition test of the sample initialized by flooding also showed a water-wet response. As illustrated in Fig. 3d, the oil droplets emerging while the brine invades the pore space show a water-wet shape. Similar observations for a Ketton rock initialized by flooding have been reported by Alyafei and Blunt (2016).

The sample initialized by centrifugation, however, showed only a little oil production from the pore space (1%) and the oil droplets accumulating at the top of the sample showed an oil-wet structure (Fig. 3c) (Bartels et al., 2017a).

The difference between the initialization by flooding and the initialization by centrifugation is the capillary pressure applied during drainage.

Based on the Young-Laplace equation, a higher capillary pressure leads to the invasion of smaller pores by oil compared to a lower capillary pressure. As the rock surface is altered in contact with the crude (Buckley, 2001), only the pores invaded by oil are expected to change wettability.

Figure 4 shows the pore- (inlet) diameter distribution of Ketton rock obtained by mercury porosimetry and the estimated pore (inlet) diameter invaded by centrifugation and flooding, respectively, for the Amott test examples (Bartels et al., 2017a). The pore sizes invaded by centrifugation were estimated based on the rotation speed, interfacial tension and fluid densities assuming an advancing contact angle of 30°. Based on this calculation, pores down to a diameter of 0.3 µm are expected to be filled with oil (Bartels et al., 2017a): this is sufficient to invade some microporosity and hence, make the solid surfaces oil-wet. As no porous plate was used during flooding the maximum capillary pressure achieved is controlled by the pore structure itself. An exact value cannot be determined. However, the capillary pressure is expected

to be at the lower end of the peak pore (inlet) diameter. µCT images obtained with the EMCT scanner after drainage were used for validation. In these images, all the resolved pore sizes showed occupancy with oil. The small amounts of water detected did not show a correlation with the pore diameter. However, it is likely that the microporosity in the grains remained water-saturated and water-wet. This is evident in the high initial water saturation of approximately 0.4 in the results shown in Fig. 3. The solid grains are microporous—if they are water-filled, they act like a wet sponge and may prevent contact of oil with the surface of the grains even in the larger pores and hence, retaining water-wet characteristics in this case. We will test this directly later in the paper by measuring water-film thicknesses in the corners of the macropore space using AFM.

Correspondingly, the estimated minimum pore radius accessed during flooding was set at 20 µm at the image resolution boundary (4 voxel lengths) and below the larger peak pore (inlet) diameter (Fig. 4). Smaller-scale imaging techniques, such as µCT and AFM, can give further insights into the core-scale wettability response and will be discussed below in more detail.

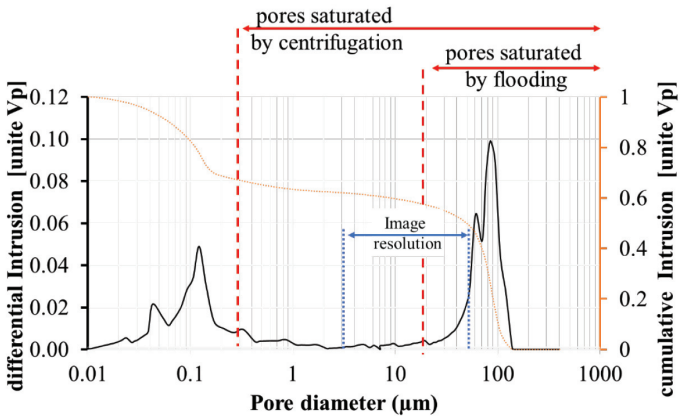

Fig. 4—Pore-size distribution of Ketton rock. Based on the oil-saturations obtained from the experiments, initialization by flooding-filled pores down to a diameter of 20 µm and centrifugation down to 0.3 µm (Bartels et al., 2017a; Rücker et al., 2020).

Wettability at the Pore Scale

The µCT unsteady-state waterflood experiments were used to compare the impact of centrifugation and flooding on sample initialization at the pore scale.

The images Figs. 5 and 6 show examples of the fluid distribution at the pore scale before and after an unsteady-state waterflood for a sample initialized by flooding (Fig. 5, measured at SLS) and by centrifugation (Fig. 6, measured with Xradia).

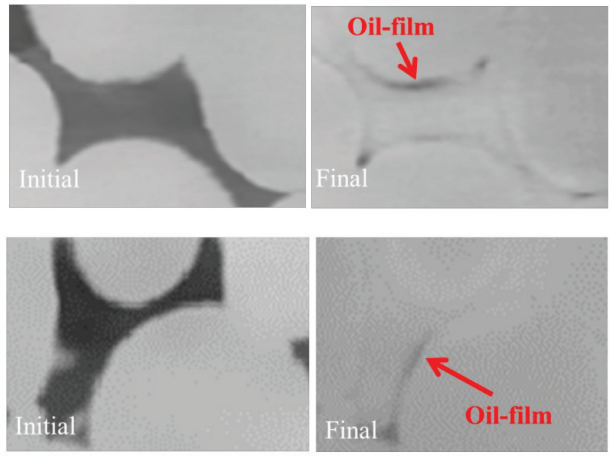

Fig. 5—µCT images obtained before (left) and after the waterflood experiment (right) of a Ketton rock sample (gray) initialized by flooding. Next to the oil (black) and brine (white), the images show the presence of emulsion (dark gray). Furthermore, the images show the presence of discontinuous oil films along the surfaces and in crevices (Rücker, 2018). The images were obtained at the SLS.

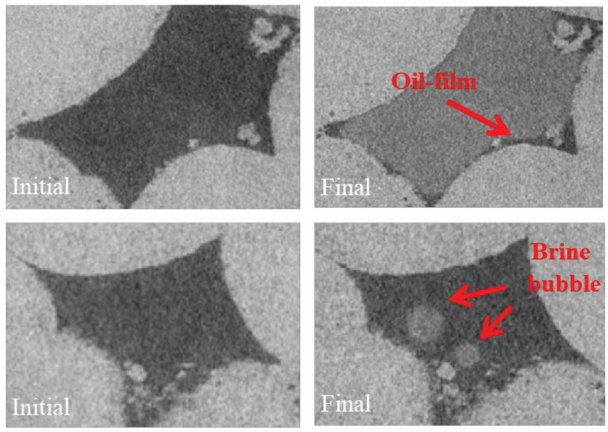

Fig. 6—µCT images obtained before (left) and after the waterflood experiment (right) of a Ketton rock sample initialized by centrifugation. The emulsion phase appears in the form of distinct brine droplets. The oil films appear continuous. The images were obtained with Xradia (Rücker, 2018).

Next to the brine phase (white), the oil phase (black) and the rock (light gray), both figures also show the presence of a water-in-oil emulsion. In the sample initialized by flooding the emulsion appears as a third phase (dark gray) (Bartels

et al., 2017b). In the sample initialized by centrifugation, the emulsion appears in distinct droplets with a diameter of up to 100 µm. The emulsion forms due to the presence of surface-active components in the crude, which are also responsible for the wettability alteration of the system itself. The identification and image processing of this third phase was discussed in detail by Bartels et al. (2017b).

Furthermore, both figures show the presence of oil films along the grain surfaces and in the crevices in between after the waterflood. However, for the centrifuged sample, this oil appears continuous, while the oil films in the flooded sample appear discontinuous (compare Figs. 5 and 6). This supports the findings observed at the core scale. The discontinuous oil films observed in the µCT images hint to a mixed-wet sample, while the continuous oil films indicate a predominantly oil-wetting surface. The difference in the emulsion phase can be explained in the same way. As the surface is oil-wet after centrifugation, large water droplets may form and remain stable, while in a mixed-wet system, larger droplets are likely to collapse as they get in contact with the preserved water films in a mixed-wet system and only small droplets, (below the image resolution) remain stable.

The images obtained at the end of each waterflood experiment were further used to measure the contact-angle distribution displayed in Fig. 7. The contact-angle distribution obtained for the Ketton sample indicates a water-wet system with a peak < 90°. However, compared to the contact-angle distribution for the strongly water-wet decane-brine-Ketton rock sample reported by Scanziani et al. (2017), this system seems shifted by 30° towards more oil-wet conditions.

Yet, the contact-angle distribution does not show the mixed-wet system observed in the image. The reason might be the patchy small-scale wettability pattern, which leads to pinning of the fluid-fluid interface when the surface changes from water-wet to oil-wet.

The contact angles detected in the sample initialized by centrifugation varied from 50° to 130°, with a median value of 115° (Fig. 7). Only 21 contact angles could be obtained for this sample. The reason was that the oil remained predominantly in the poorly resolved pore throats, which are less suitable for contact-angle measurements. For the same reason, the contact angles obtained may be more affected by measurement errors, which needs to be considered for the following interpretation: The low values of 50° might be a sign of a mixed-wettability pattern. However, as the oil-phase in this sample is continuous, the pinning of the fluid-fluid interface is less pronounced.

The sample initialization of the two cores investigated was subject to different capillary pressures applied during the drainage process and aging time. However, the impact of aging time was assumed to be minor for the following reasons. First, the core-scale studies indicate that the wettability alteration of Ketton rock appears already after 24 hours. Second, previous studies indicated that the

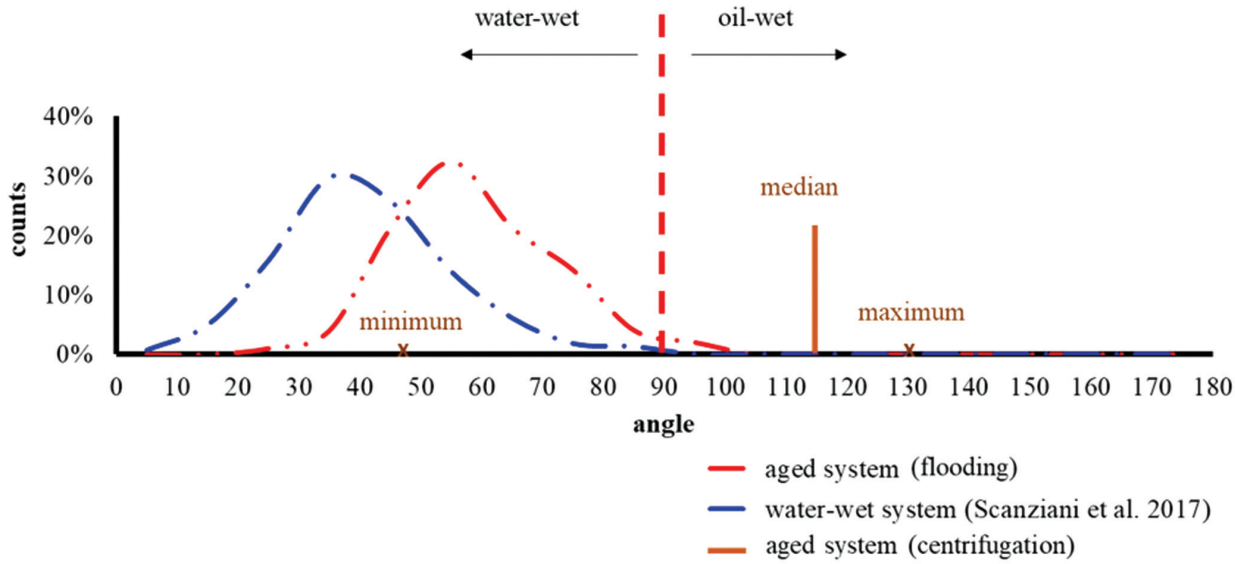

Fig. 7—The contact-angle distribution (100 contact angles) for the unsteady-state waterflood µCT experiment with a rock sample initialized by flooding indicates a water-wet state even though more oil-wet than the water-wet reference obtained from Scanziani et al. (2017). Due to the low number of contact angles (21 contact angles) obtained for the unsteady-state waterflood µCT experiment performed on a centrifuged sample flooding, solely the median value, the maximum and minimum are plotted (Rücker, 2018; Rücker et al., 2019a).

water-wet appearance of Ketton rock is preserved for even longer aging periods (Alyafei and Blunt, 2016). Third, oil layers, present in the flooded sample, show that wettability alteration happened where the oil was in contact with the surface. The oil layer, however, was discontinuous, which might have been caused by subresolution surface features, which can be investigated with AFM.

Wettability at the Subpore Scale

AFM was used to investigate the water films and layers present within the Ketton rock sample initialized by flooding.

The water-decane interface and the height of the rock surface were obtained from the force-distance curves collected for all of the 128×128 pixels along the 10 µm × 10 µm area. Figure 8 shows examples for such force-distance curves obtained from measurements on calcite surfaces prepared with and without water.

As the tip is water-wet, the cantilever bends towards the surface when it passes through the fluid-fluid interface during the approach, which is displayed in form of a negative force. The height of the rock surface is obtained from the bending of the tip in the opposite direction recorded as a positive force on the cantilever.

In the resulting image, shown in Fig. 9, 60% of the surface was covered with brine. Only 40% of the surface was directly in contact with decane.

The 3D measurement of the wetting film also allows the quantification of fluid-film thickness. Figure 9b shows that the film thickness ranges between 0 and 200 nm with a peak film thickness of 125 nm. The observed water-film thickness is a result of disjoining pressure, capillary pressure and surface topography (Kovscek et al., 1993; Rücker et al., 2020). The film breaks along the hills of the surface, but remains intact within asperities (Schmatz et al., 2015; Rücker et al., 2020).

Furthermore, the rock surface obtained was used to simulate the coverage of the rock for different capillary pressures applied using a morphological drainage simulation. The algorithm fits spheres of different radii, representing different capillary pressures, onto the surface to model the drainage process as it is applied prior to the wettability alteration in a rock.

The result is shown in Fig. 10. Figure 10d shows the surface area coverage as a function of sphere diameter. The higher the diameter—and the lower the corresponding capillary pressure—the larger the surface area covered with brine. Fifty percent of the surface was covered with water for a sphere diameter of 7 µm. For sphere diameters below

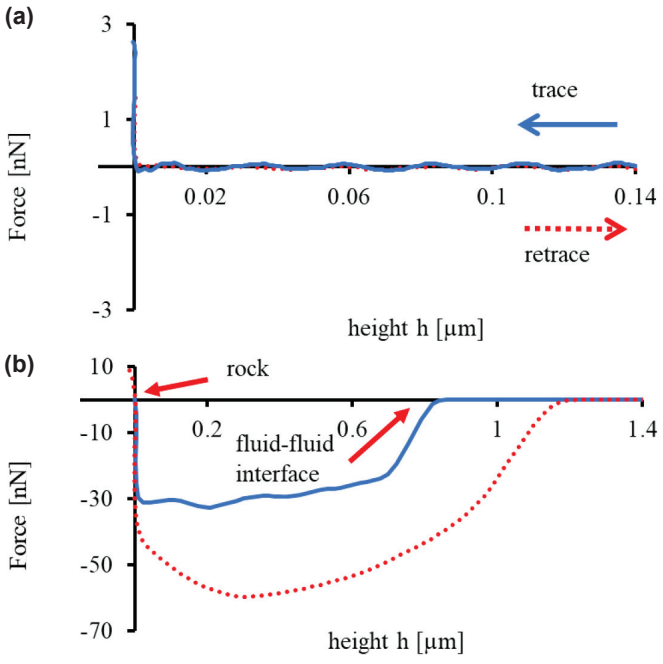

Fig. 8—Representative force-distance curves obtained from a calcite surface without (a) and with the presence of a water film (b). As the tip passes through the brine-decane interface, the cantilever is bending towards the surface, which is recorded as a negative force. Once the cantilever reaches the rock surface it gets bent in the opposite direction (Rücker, 2018).

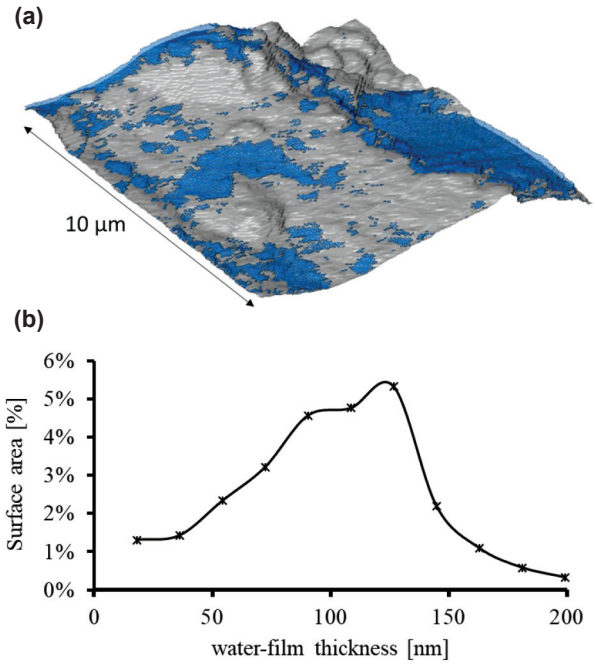

Fig. 9—(a) Water film (blue) on top of a rock surface (gray) measured in decane. (b) The water layer shows a film thickness ranging between 0 and 200 nm with a peak film thickness of 125 nm (Rücker, 2018).

1.5 µm only 1.5% of the surface remained in contact with the aqueous phase. These results are in line with the detected water films.

These findings show that surface roughness of a rock can facilitate the formation of water-layers. Different capillary pressures applied on the rock during drainage result in different water coverage of the rock surface (Rücker et al., 2020). Based on the assumption that wettability alteration occurs predominantly when the surface is in direct contact with the oil, the difference in coverage would result in a subpore-scale wettability pattern, as indicated in the previous section on Wettability at the Pore Scale, and explain the different wettability responses observed at the core-scale.

CONCLUSIONS

In this study we assessed the wettability across length scales using asimilar oil-brine-rock systems, including AFM at the subpore scale, µCT imaging and contact-angle distributions at the pore scale combined with Amott spontaneous imbibition tests and steady-state relative permeability measurements at the core scale, demonstrating that upscaling is possible.

For this crude-oil-brine-rock system, surface roughness and the capillary pressure applied during initialization were found to control the larger-scale wettability response after ageing.

AFM studies showed the formation of water films along the rock surface, preventing direct contact of the oil and the rock which lead to a patchy subpore scale wettability pattern after aging. This small-scale wettability pattern leads to a water-wet contact-angle distribution at the pore scale, while some surfaces show discontinuous oil layers and a mixed-wet core-scale response leaning towards the water-wet side. Furthermore, nanoscale simulations showed that the higher the capillary pressure, the larger the oil-rock contact area. Once the oil film becomes continuous the core-scale response for the same system appears oil-wet at the pore and core scales.

This study demonstrates that for predictions of the core-scale wettability response, the nanoscale surface structure of the rock needs to be considered.

ACKNOWLEDGEMENTS

We would like to acknowledge the staff of UGCT, Ghent, Belgium, for support for the spontaneous imbibition experiment and the Paul Scherrer Institute, Villigen, Switzerland, for the provision of synchrotron radiation beamtime at TOMCAT beamline of the SLS and for assistance during the session. Furthermore, we would like to thank Anne Bonnin, Christian Hinz, Arne Jacob, Christian Wagner, Steven Henkel and Frieder Enzmann for support during the beamline experiments. We would like to acknowledge Alex Schwing and Rob Neiteler for the design of the setup and instrumentation, Fons Marcelis for sample preparation, Holger Ott, Ryan Armstrong and James McClure, Alex Winkel, Hayley Meek, Matthew

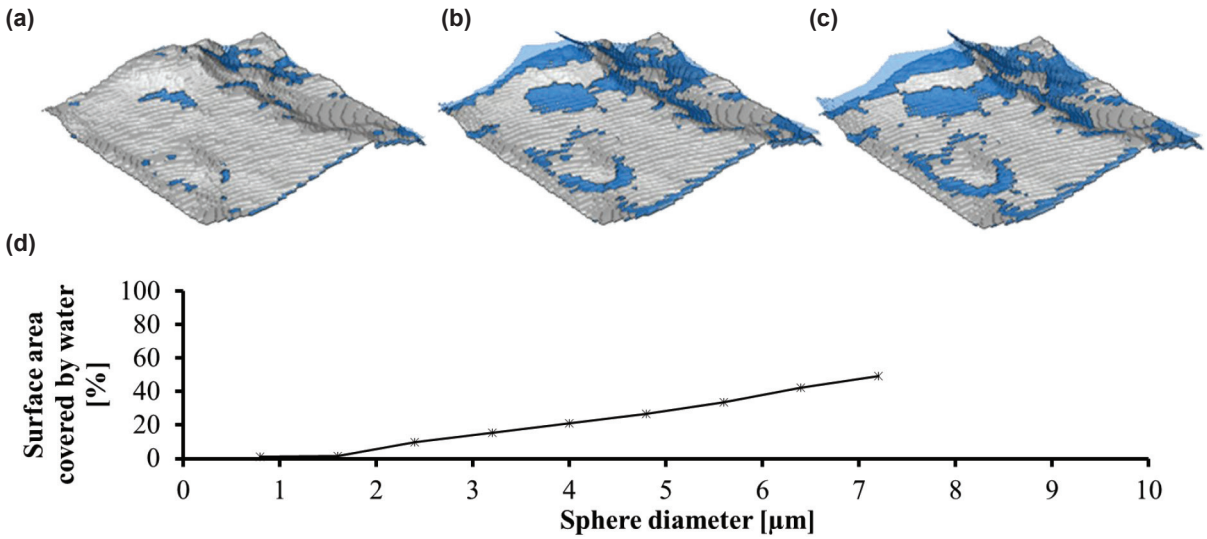

Fig. 10—Water films (blue) on top of a rock surface (gray) obtained from a drainage simulation based on sphere fitting (a) sphere diameter = 1.6 µm, (b) sphere diameter = 5.6 µm, (c) sphere diameter = 6 µm). (d) shows the percentage of surface area covered with brine as a function of sphere diameter (Rücker, 2018).

Leivers, Tannaz Pak, the Shell Digital Rock team at Imperial and the team from Math2Market for helpful discussions. Tom Bultreys is a post-doctoral fellow of the Research Foundation-Flanders (FWO) and acknowledges its support under grant 12X0919N. We gratefully acknowledge Shell Global Solutions International B.V. for their permission to publish this work.

Spontaneous imbibition data are available from Bartels et al. (2019b) and forced imbibition data from (Rücker et al., 2019b): https://www.digitalrocksportal.org/projects/188 , https://www.digitalrocksportal.org/projects/202.

NOMENCLATURE

Abbreviations

AFM = atomic-force microscopy
FW = fresh water
HS = high salinity
SARA = saturate, aromatics, resins, asphaltenes
SCAL = special core analysis
TAN = total acid number
TBN = total base number
μCT = microcomputed tomography

Symbols

d = diameter
f_w = water fraction
k_{rw} = relative permeability of water
k_{ro} = relative permeability of oil
L = length
P = pressure
S = saturation
T = temperature
θ = contact angle

REFERENCES

Abdallah, W., Buckley, J.S., Carnegie, A., Edwards, J., Herold, B., Fordham, E., Graue, A., Habashy, T., Seleznev, N., Signer, C., Hussain, H., Montaron, B., and Ziauddin, M., 2007, Fundamentals of Wettability, *Schlumberger Oilfield Review*, **19**(2), 44–61.

Akhlaq, M.S., Kessel, D., and Dornow, W., 1996, Separation and Chemical Characterization of Wetting Crude Oil Compounds, *Journal of Colloid and Interface Science*, **180**(2), 309–314. DOI. 10.1006/jcis.1996.0308.

Al-Raoush, R.I., 2009, Impact of Wettability on Pore-Scale Characteristics of Residual Nonaqueous Phase Liquids, *Environmental Science & Technology*, **43**(13), 4796–4801. DOI: 10.1021/es802566s.

Alhammadi, A.M., Alratrout, A., Singh, K., Bijeljic, B., and Blunt, M.J., 2017, In Situ Characterization Of Mixed–Wettability In A Reservoir Rock At Subsurface Conditions, *Scientific Reports*, **7**(1), 10753. DOI: 10.1038/s41598-017-10992-w.

AlRatrout, A., Raeini, A.Q., Bijeljic, B., and Blunt, M.J., 2017, Automatic Measurement of Contact Angle in Pore-Space Images, *Advances in Water Resources*, **109**, 158–169. DOI: 10.1016/j.advwatres.2017.07.018.

Alyafei, N., and Blunt, M.J., 2016, The Effect of Wettability on Capillary Trapping in Carbonates: *Advances in Water Resources*, **90**(Supplement C), 36–50. DOI: 10.1016/j.advwatres.2016.02.001.

Amott, E., 1959, Observations Relating to the Wettability of Porous Rock, Paper SPE-1167-G, *Transactions, AIME*, **216**, 156–162. DOI: 10.2118/1167-G.

Anderson, W., 1986, Wettability Literature Survey—Part 1: Rock/Oil/Brine Interactions and the Effects of Core Handling on Wettability, Paper SPE-13932, *Journal of Petroleum Technology*, **38**(10), 1125–1144. DOI: 10.2118/13932-PA.

Anderson, W., 1987a, Wettability Literature Survey—Part 4: Effects of Wettability on Capillary Pressure, Paper SPE-15271, *Journal of Petroleum Technology*, **39**(10), 1283–1300. DOI: 10.2118/15271-PA.

Anderson, W., 1987b, Wettability Literature Survey Part 5: The Effects of Wettability on Relative Permeability, Paper SPE-16323, *Journal of Petroleum Technology*, **39**(11), 1453–1468. DOI: 10.2118/16323-PA.

Andrew, M., 2015, Reservoir-Condition Pore-Scale Imaging of Multiphase Flow, unpublished PhD dissertation, Imperial College London. DOI: 10.25560/24915, URL: http://hdl.handle.net/10044/1/24915.

Andrew, M., Bijeljic, B., and Blunt, M.J., 2014, Pore-Scale Contact Angle Measurements at Reservoir Conditions Using X-Ray Microtomography, *Advances in Water Resources*, **68,** 24–31. DOI: 10.1016/j.advwatres.2014.02.014.

Andrew, M., Menke, H., Blunt, M.J., and Bijeljic, B., 2015, The Imaging of Dynamic Multiphase Fluid Flow Using Synchrotron-Based X-Ray Microtomography at Reservoir Conditions, *Transport in Porous Media*, **110**(1), 1–24. DOI: 10.1007/s11242-015-0553-2

Arganda-Carreras, I., Kaynig, V., Rueden, C., Eliceiri, K.W., Schindelin, J., Cardona, A., and Sebastian Seung, H., 2017, Trainable Weka Segmentation: A Machine Learning Tool for Microscopy Pixel Classification, *Bioinformatics*, **33**(15), 2424–2426. DOI: 10.1093/bioinformatics/btx180.

Armstrong, R.T., Mcclure, J.E., Robins, V., Liu, Z., Arns, C.H., Schlüter, S., and Berg, S., 2018, Porous Media Characterization Using Minkowski Functionals: Theories, Applications and Future Directions, *Transport in Porous Media*, **130**(1), 305–335. DOI: 10.1007/s11242-018-1201-4.

Armstrong, R.T., Ott, H., Georgiadis, A., Rücker, M., Schwing, A., and Berg, S., 2014, Subsecond Pore-Scale Displacement Processes and Relaxation Dynamics in Multiphase Flow, *Water Resources Research*, **50**(12), 9162–9176. DOI: 10.1002/2014WR015858.

Armstrong, R.T., Porter, M.L., and Wildenschild, D., 2012, Linking Pore-Scale Interfacial Curvature to Column-Scale Capillary Pressure, *Advances in Water Resources*, **46**, 55–62.

DOI: 10.1016/j.advwatres.2012.05.009.

Bartels, W., 2018, Pore Scale Processes in Mixed-Wet Systems With Application io Low Salinity Waterflooding, unpublished PhD dissertation, Utrecht University Department of Earth Sciences. ISBN: 978-90-6266-497-9. URL: https://dspace.library.uu.nl/bitstream/handle/1874/362302/Bartels.pdf?sequence=1&isAllowed=y. Accessed March 5, 2020.

Bartels, W.B., Mahani, H., Berg, S., and Hassanizadeh, S.M., 2019a, Literature Review of Low Salinity Waterflooding From a Length and Time Scale Perspective, *Fuel*, **236**, 338–353. DOI: 10.1016/j.fuel.2018.09.018.

Bartels, W.B., Rücker, M., Berg, S., Mahani, H., Georgiadis, A., Fadili, A., Brussee, N., Coorn, A., Van Der Linde, H., Hinz, C., Jacob, A. Wagner, C. Henkel, S., Enzman, F., Bonnin, A., Stampanoni, M., Ott, H., Blunt, M., and Hassanizadeh, S.M., 2017b, Fast X-Ray Micro-CT Study of the Impact of Brine Salinity on the Pore-Scale Fluid Distribution During Waterflooding, *Petrophysics*, **58**(1), 36–47.

Bartels, W.B., Rücker, M., Boone, M., Bultreys, T., and Cnudde, V., 2019b, Micro-CT Datasets for Spontaneous Imbibition Experiments on SCAL and Mini-Plugs, Digital Rocks Portal. URL: https://www.digitalrocksportal.org.

Bartels, W., Rücker, M., Boone, M., Bultreys, T., Mahani, H., Berg, S., Hassanizadeh, S., and Cnudde, V., 2017a, Pore-Scale Displacement During Fast Imaging of Spontaneous Imbibition, Paper SCA2017-005 presented at the International Symposium of the Society of Core Analysts, Vienna, Austria, 27 August–1 September.

Benner, F.C., Riches, W.W., and Bartell, F.E., 1938, Nature and Importance of Surface Forces in Production of Petroleum, Paper API-38-442 presented at the API Drilling and Production Practice Conference, Amarillo, Texas, 17–18 February

Berg, S., Cense, A.W., Hofman, J.P., and Smits, R.M.M., 2008, Two-Phase Flow in Porous Media With Slip Boundary Condition, *Transport in Porous Media*, **74**(3), 275–292. DOI: 10.1007/s11242-007-9194-4.

Berg, S., Rücker, M., Ott, H., Georgiadis, A., Van Der Linde, H., Enzmann, F., Kersten, M., Armstrong, R., De With, S., Becker, J., and Wiegmann, A., 2016, Connected Pathway Relative Permeability From Pore-Scale Imaging of Imbibition, *Advances in Water Resources*, **90**, 24–35. DOI: 10.1016/j.advwatres.2016.01.010.

Blunt, M.J., 2017, *Multiphase Flow in Permeable Media: A Pore-Scale Perspective*, Cambridge University Press. ISBN: 978-01107093461.

Broseta, D., Tonnet, N., and Shah, V., 2012, Are Rocks Still Water-Wet in the Presence of Dense CO_2 or H_2S?, *Geofluids*, **12**(4), 280–294. DOI: 10.1111/j.1468-8123.2012.00369.x.

Brown, R.J.S., and Fatt, I., 1956, Measurements of Fractional Wettability of Oil Fields' Rocks by the Nuclear Magnetic Relaxation Method, Paper SPE-743-G presented at the Fall Meeting of the Petroleum Branch of AIME: Los Angeles, California, USA, 14–17, October. DOI: 10.2118/743-G.

Buckley, J.S., 2001, Effective Wettability of Minerals Exposed to Crude Oi, *Current Opinion In Colloid & Interface Science*, **6**(3), 191–196. DOI: 10.1016/S1359-0294(01)00083-8.

Buckley, J.S., Bousseau, C., and Liu, Y., 1996, Wetting Alteration by Brine and Crude Oil: From Contact Angles to Cores, Paper SPE-30765, *SPE Journal*, **1**(30), 341–350. DOI: 10.2118/30765-PA.

Buckley, J.S., Liu, Y., Xie, and Morrow, N.R., 1997, Asphaltenes and Crude Oil Wetting—The Effect of Oil Composition, Paper SPE-35366, *SPE Journal*, **2**(2), 107–119. DOI: 10.2118/35366-PA.

Bultreys, T., De Boever, W., and Cnudde, V., 2016, Imaging And Image-Based Fluid Transport Modeling at the Pore Scale in Geological Materials: A Practical Introduction to the Current State-of-the-Art, *Earth-Science Reviews*, **155**, 93–128. DOI: 10.1016/j.earscirev.2016.02.001.

Bultreys, T., Lin, Q., Gao, Y., Raeini, A.Q., Alratrout, A., Bijeljic, B., and Blunt, M.J., 2018, Validation of Model Predictions of Pore-Scale Fluid Distributions During Two-Phase Flow, *Physical Review E*, **97**(5), 053104. DOI: 10.1103/PhysRevE.97.053104.

Dake, L., 1983, *Fundamentals of Reservoir Engineering*, 1st Edition, Elsevier. ISBN: 978-044448302.

Deng, Y., Xu, L., Lu, H., Wang, H., and Shi, Y., 2018, Direct Measurement of the Contact Angle of Water Droplet on Quartz in a Reservoir Rock With Atomic Force Microscopy, *Chemical Engineering Science*, **177**, 445–454. DOI: 10.1016/j.ces.2017.12.002.

Derjaguin, B., and Landau, L., 1941, Theory of the Stability of Strongly Charged Lyophobic Sols and of the Adhesion of Strongly Charged Particles in Solutions of Electrolytes: *Acta Physico Chimica URSS*, **14**(633). Reprinted in 1993, *Progress in Surface Science*, **43**(1–4), 30–59. DOI: 10.1016/0079-6816(93)90013-L.

Donaldson, E.C., and Alam, W., 2008a, Wettability, Chapter 1 *in Wettability*, Gulf Publishing Company, 1–55. ISBN: 978-1-933762-29-6.

Donaldson, E.C., and Alam, W., 2008b, Wettability and Production, Chapter 3 *in Wettability*, Gulf Publishing Company, 121–172. ISBN: 978-1-933762-29-6.

Donaldson, E.C., Thomas, R.D., and Lorenz, P.B., 1969, Wettability Determination and its Effect on Recovery Efficiency, Paper SPE-2338, *SPE Journal*, **9**(1), 13–20. DOI: 10.2118/2338-PA.

Drummond, C., and Israelachvili, J., 2004, Fundamental Studies of Crude Oil-Surface Water Interactions and its Relationship to Reservoir Wettability, *Journal of Petroleum Science and Engineering*, **45**(1–20), 61–81. DOI: 0.1016/j.petrol.2004.04.007.

Fan, T., Wang, J., and Buckley, J.S., 2002, Evaluating Crude Oils by SARA Analysis, Paper SPE-75228 presented at the SPE/DOE Improved Oil Recovery Symposium, Tulsa, Oklahoma, 13–17 April. DOI: 10.2118/75228-MS.

Fernø, M.A., Torsvik, M., Haugland, S., and Graue, A., 2010, Dynamic Laboratory Wettability Alteration, *Energy & Fuels*, **24**(7), 3950–3958. DOI: 10.1021/ef1001716.

Flügel, E., 2004, Microfacies of Carbonate Rocks: Analysis, Interpretation and Application, Springer-Verlag. DOI: 10.1007/978-3-662-08726-8.

Fogden, A., 2011, Effect of Water Salinity and pH on the Wettability of a Model Substrate, *Energy & Fuels*, **25**(11), 5113–5125. DOI: 10.1021/ef200920s.

Giro, R., Bryant, P.W., Engel, M., Neumann, R.F., and Steiner, M.B., 2017, Adsorption Energy as a Metric for Wettability at the Nanoscale, *Scientific Reports*, **7**, 46317. DOI: 10.1038/srep46317.

Hassenkam, T., Andersson, M.P., Hilner, E., Matthiesen, J., Dobberschütz, S., Dalby, K.N., Bovet, N., Stipp, S.L., Salino, P., Reddick, C., and Collins, I.R., 2015, Could Atomic-Force Microscopy Force Mapping be a Fast Alternative to Core-Plug Tests for Optimizing Injection-Water Salinity for Enhanced Oil Recovery in Sandstone?, Paper SPE-169136, *SPE Journal*, **21**(3), 720–729. DOI: 10.2118/169136-PA.

Hassenkam, T., Skovbjerg, L.L., and Stipp, S.L.S., 2009, Probing the Intrinsically Oil-Wet Surfaces of Pores in North Sea Chalk at Subpore Resolution, *Proceedings of the National Academy of Sciences*, **106**(15), 6071–6076. DOI: 10.1073/pnas.0901051106.

Herminghaus, S., 2000, Roughness-Induced Non-Wetting, *Europhysics Letters*, **52**(2), 165–170. DOI: 10.1209/epi/i2000-00418-8.

Herring, A.L., Harper, E.J., Andersson, L., Sheppard, A., Bay, B.K., and Wildenschild, D., 2013, Effect of Fluid Topology on Residual Nonwetting Phase Trapping: Implications for Geologic CO_2 Sequestration, *Advances in Water Resources*, **62**, Part A, 47–58. DOI: 10.1016/j.adwatres.2013.09.015.

Herring, A.L., Middleton, J., Walsh, R., Kingston, A., and Sheppard, A., 2017, Flow Rate Impacts on Capillary Pressure and Interface Curvature of Connected and Disconnected Fluid Phases During Multiphase Flow in Sandstone, *Advances In Water Resources*, **107**, 460–469. DOI: 10.1016/j.advwatres.2017.05.011.

Herring, A.L., Sheppard, A., Andersson, L., and Wildenschild, D., 2016, Impact of Wettability Alteration on 3D Nonwetting Phase Trapping and Transport, *International Journal of Greenhouse Gas Control*, **46**, 175–186. DOI: 10.1016/j.ijggc.2015.12.026.

Hilpert, M., and Miller, C.T., 2001, Pore-Morphology-Based Simulation of Drainage in Totally Wetting Porous Media, *Advances in Water Resources*, **24**(3), 243–255. DOI: 10.1016/S0309-1708(00)00056-7.

Hirasaki, G.J., 1991, Wettability: Fundamentals and Surface Forces, Paper SPE-17367, *SPE Formation Evaluation*, **6**(2), 217–226. DOI: 10.2118/17367-PA.

Hjelmeland, O.S., and Larrondo, L.E., 1986, Experimental Investigation of the Effects of Temperature, Pressure, and Crude Oil Composition on Interfacial Properties, Paper SPE-12124, *SPE Reservoir Engineering*, **1**(4), 321–328. DOI: 10.2118/12124-PA.

Iglauer, S., Fernø, M., Shearing, P., and Blunt, M., 2012, Comparison of Residual Oil Cluster Size Distribution, Morphology and Saturation in Oil-Wet and Water-Wet Sandstone, *Journal of Colloid and Interface Science*, **375**(1), 187–192. DOI: 10.1016/j.jcis.2012.02.025.

Israelachvili, J.N., 2011, Adhesion and Wetting Phenomena, Chapter 17 *in Intermolecular and Surface Forces*, 3rd Edition, Academic Press, 415–467. DOI: 1016/C2009-0-21560-1.

Joekar-Niasar, V., Hassanizadeh, S.M., and Leijnse, A., 2008, Insights Into the Relationships Among Capillary Pressure, Saturation, Interfacial Area and Relative Permeability Using Pore-Network Modeling, *Transport In Porous Media*, **74**(2), 201–219. DOI: 10.1007/s11242-007-9191-7.

Kokkedee, J., Boom, W., Frens, A., and Maas, J., 1996, Improved Special Core Analysis: Scope for a Reduced Residual Oil Saturation, PaperSCA9601 presented at the International Sympsoium of the Society of Core Analysis, Montpellier, France.

Kovscek, A.R., Wong, H., and Radke, C.J., 1993, A Pore-Level Scenario for the Development of Mixed Wettability in Oil Reservoirs, *AIChE Journal*, **39**(6), 1072–1085. DOI: 10.1002/aic.690390616.

Kumar, K., Dao, E., and Mohanty, K., 2005, Atomic Force Microscopy Study of Wettability Alteration, Paper SPE-93009 presented at the SPE International Symposium on Oilfield Chemistry, The Woodlands, Texas, USA, 2–4 February. DOI: 10.2218/93009-MS.

Leach, R.O., Wagner, O.R., Wood, H.W., and Harpke, C.F., 1962, A Laboratory and Field Study of Wettability Adjustment in Water Flooding, Paper SPE-119, *Journal of Petroleum Technology*, **14**(2), 206–212. DOI: 10.2118/119-PA.

Lehmann, P., Berchtold, M., Ahrenholz, B., Tölke, J., Kaestner, A., Krafczyk, M., Flühler, H., and Künsch, H. R., 2008, Impact of Geometrical Properties on Permeability and Fluid Phase Distribution in Porous Media, *Advances in Water Resources*, **31**(9), 1188–1204. DOI: 10.1016/j.advwatres.2008.01.019.

Leverett, M.C., 1941, Capillary Behavior in Porous Solids, Paper SPE-941152-G, *Transactions, AIME*, **142**, 152–169. DOI: 10.2118/941152-G.

Lin, Q., Bijeljic, B., Berg, S., Pini, R., Blunt, M.J., and Krevor, S., 2019a, Minimal Surfaces in Porous Media: Pore-Scale Imaging of Multiphase Flow in an Altered-Wettability Bentheimer Sandstone, *Physical Review E*, **99**(6), 063105. DOI: 10.1103/PhysRevE.99.063105.

Lin, Q., Bijeljic, B., Krevor, S.C., Blunt, M.J., Rücker, M., Berg, S., Coorn, A., Van Der Linde, H., Georgiadis, A., and Wilson, O.B., 2019b, A New Waterflood Initialization Protocol With Wettability Alteration for Pore-Scale Multiphase Flow Experiments, *Petrophysics*, **60**(2), 264–272. DOI: 10.30632/PJV60N2-2019a4.

Lin, Q., Bijeljic, B., Pini, R., Blunt, M.J., and Krevor, S., 2018, Imaging and Measurement of Pore-Scale Interfacial Curvature to Determine Capillary Pressure Simultaneously With Relative Permeability, *Water Resources Research*, **54**(9), 7046–7060. DOI: 10.1029/2018/WR023214.

Ma, S., Morrow, N., and Zhang, X., 1997, Generalized Scaling of Spontaneous Imbibition Data for Strongly Water-Wet Systems, *Journal of Petroleum Science and Engineering*, **18**(3–4), 165–178. DOI: 10.1016/S0920-4105(97)00020-X.

Mahani, H., Keya, A.L., Berg, S., Bartels, W.-B., Nasralla, R., and Rossen, W.R., 2015, Insights into the Mechanism of Wettability Alteration by Low-Salinity Flooding (LSF) in Carbonates, *Energy & Fuels*, **29**(3), 1352–1367. DOI: 10.1021/ef5023847.

Mahani, H., Menezes, R., Berg, S., Fadili, A., Nasralla, R., Voskov, D., and Joekar-Niasar, V., 2017, Insights into the Impact of Temperature on the Wettability Alteration by Low Salinity in

Carbonate Rocks, *Energy & Fuels*, **31**(8), 7839–7853. DOI: 10.1021/acs.energyfuels.7b00776.

Masschaele, B., Dierick, M., Loo, D.V., Boone, M.N., Brabant, L., Pauwels, E., van Hoorebeke, L., and Cnudde, V., 2013, HECTOR: A 240kV Micro-CT Setup Optimized for Research, *Journal of Physics: Conference Series*, **463**(1), 012012. DOI: 10.1088/1742-6596/463/1/012012.

Mattax, C.C., and Kyte, J., 1962, Imbibition Oil Recovery From Fractured, Water-Drive Reservoir, Paper SPE-187, *SPE Journal*, **2**(2), 177–184. DOI: 10.2118/187-PA.

Matthiesen, J., Bovet, N., Hilner, E., Andersson, M.P., Schmidt, D.A., Webb, K.J., Dalby, K.N., Hassenkam, T., Crouch, J., Collins, I.R., and Stipp, S.L.S., 2014, How Naturally Adsorbed Material on Minerals Affects Low Salinity Enhanced Oil Recovery, *Energy & Fuels*, **28**(80), 4849–4858. DOI: 10.1021/ef500218x.

McCaffery, F.G., and Mungan, N., 1970, Contact Angle and Interfacial Tension Studies of Some Hydrocarbon-Water-Solid Systems, Paper PETSOC-70-03-04, *Journal of Canadian Petroleum Technology*, **9**(3), 185–196. DOI: 10.2118/70-03-04.

McPhee, C., Reed, J., and Zubizarreta, I., 2015*, Core Analysis: A Best Practice Guide*, Elsevier. ISBN: 978-0444635334.

Mennella, A., Morrow, N.R., and Xie, X., 1995, Application of the Dynamic Wilhelmy Plate to Identification of Slippage at a Liquid-Liquid-Solid Three-Phase Line of Contact, *Journal of Petroleum Science and Engineering*, **13**(3–4), 179–192. DOI: 10.1016/0920-4105(05)00009-7.

Morrow, N.R., 1975, The Effects of Surface Roughness on Contact: Angle With Special Reference to Petroleum Recovery, Paper PETSOC-75-04-04, *Journal of Canadian Petroleum Technology*, **14**(4). DOI: 10.2118/75-04-04.

Neumann, A.W., and Good, R.J., 1979, Techniques of Measuring Contact Angles,Chapter 2 *in* Good, R.J., and Stromberg, R.R., Eds., *Surface and Colloid Science*, **11**, Springer, 31–91. DOI: 10.1007/978-1-4615-7969-4_2.

Paganin, D., Mayo, S., Gureyev, T.E., Miller, P.R., and Wilkins, S.W., 2002, Simultaneous Phase and Amplitude Extraction From a Single Defocused Image of a Homogeneous Object, *Journal of Microscopy*, **206**(1), 33–40. DOI: 10.1046/j.1365-2818.2002.01010.x.

Purswani, P., Tawfik, M.S., and Karpyn, Z.T., 2017, Factors and Mechanisms Governing Wettability Alteration by Chemically Tuned Waterflooding: A Review, *Energy & Fuels*, **31**(8), 7734–7745. DOI: 10.1021/acs.eneryfuels.7b01067.

Quéré, D., 2008, Wetting and Roughness, *Annual Review of Materials Research*, **38**, 71–99. DOI: 10.1146/annurev.matsci.38.060407.132434.

Rücker, M., 2018, Wettability and Wettability Alteration at the Pore- and Nano- Scales, unpublished PhD dissertation, Imperial College London. DOI: 10.25560/66307. URL: http://hdl.handle.net/10044/1/66307

Rücker, M., Bartels, W.-B., Singh, K., Brussee, N., Coorn, A., Van Der Linde, H. A., Bonnin, A., Ott, H., Hassanizadeh, S.M., Blunt, M.J., Mahani, H., Georgiadis, A., and Berg, S., 2019a, The Effect of Mixed Wettability on Pore-Scale Flow Regimes Based on a Flooding Experiment in Ketton Limestone: *Geophysical Research Letters*, **46**(6), 3225–3234. DOI: 10.1029/2018GL081784.

Rücker, M., Bartels, W., Berg, S., Enzmann, F., Jacob, A., Mahani, H., Brussee, N., Hinz, C., Georgiadis, A., and Wagner, C., 2019b, A Time-Resolved Synchrotron X-Ray Micro-Tomography Dataset of a Waterflood in an Altered Mixed-Wet Ketton Limestone, *Digital Rocks Portal*. URL: https://www.digitalrocksportal.org/projects/202. Accessed March 6, 2020.

Rücker, M., Bartels, W. B., Garfi, G., Shams, M., Bultreys, T., Boone, M., Pieterse, S., Maitland, G.C., Krevor, S., Cnudde, V., Mahani, H., Berg, S., Georgiadis, A., and Luckham, P.F., 2020, Relationship Between Wetting and Capillary Pressure in a Crude Oil/Brine/Rock System: From Nano-Scale to Core-Scale, *Journal of Colloid and Interface Science*, **562**, 159–169. DOI: 10.1016/j.jcis.2019.11.086.

Salathiel, R.A., 1973, Oil Recovery by Surface Film Drainage in Mixed-Wettability Rocks, Paper SPE-4104, *Journal of Petroleum Technology*, **25**(10), 1216–1224. DOI: 10.2118/4104-PA.

Santiso, E.E., Herdes, C., and Müller, E.A., 2013, On the Calculation of Solid-Fluid Contact Angles From Molecular Dynamics, *Entropy*, **15**(9), 3734–3745. DOI: 10.3390/e15093734.

Scanziani, A., Singh, K., Blunt, M.J., and Guadagnini, A., 2017, Automatic Method for Estimation of In Situ Effective Contact Angle From X-Ray Micro Tomography Images of Two-Phase Flow in Porous Media, *Journal of Colloid and Interface Science*, **496**, 51–59. DOI: 10.1016/j.jcis.2017.02.0005.

Schindelin, J., Arganda-Carreras, I., Frise, E., Kaynig, V., Longair, M., Pietzsch, T., Preibisch, S., Rueden, C., Saalfeld, S., Schmid, B., Tinevez, J.-Y., White, D. J., Hartenstein, V., Eliceiri, K., Tomancak, P., and Cardona, A., 2012, Fiji: An Open-Source Platform for Biological-Image Analysis, *Nature Methods*, **9**, 676–682. DOI: 10.1038/nmeth.2019

Schlüter, S., Berg, S., Rücker, M., Armstrong, R.T., Vogel, H.J., Hilfer, R., and Wildenschild, D., 2016, Pore-Scale Displacement Mechanisms as a Source of Hysteresis for Two-Phase Flow in Porous Media: *Water Resources Research*, **52**(3), 2194–2205. DOI: 10/1002/2015WR018254.

Schmatz, J., Urai, J.L., Berg, S., and Ott, H., 2015, Nanoscale Imaging of Pore-Scale Fluid-Fluid-Solid Contacts in Sandstone, *Geophysical Research Letters*, **42**(7), 2189–2195. DOI: 10.1002/2015GL063354.

Schmid, K.S., and Geiger, S., 2013, Universal Scaling of Spontaneous Imbibition for Arbitrary Petrophysical Properties: Water-Wet and Mixed-Wet States and Handy's Conjecture, *Journal of Petroleum Science and Engineering*, **101**, 44–61. DOI: 10.1016/j.petrol.2012.11.015.

Singh, K., Bijeljic, B., and Blunt, M.J., 2016, Imaging of Oil Layers, Curvature and Contact Angle in a Mixed-Wet and a Water-Wet Carbonate Rock, *Water Resources Research*, **52**(3), 1716–1728. DOI: 10/1002/2015WR018072.

Singh, K., Menke, H., Andrew, M., Lin, Q., Rau, C., Blunt, M.J., and Bijeljic, B., 2017, Dynamics of Snap-Off and Pore-Filling Events During Two-Phase Fluid Flow in Permeable Media: *Scientific Reports*, **7**, 5192. DOI: 10.1038/s41598-017-05204-4.

Treiber, L.E., and Owens, W.W., 1972, A Laboratory Evaluation of

the Wettability of Fifty Oil-Producing Reservoirs, Paper SPE-3526, *SPE Journal*, **12**(6), 531–540. DOI: 10.2118/3526-PA.

Verwey, E., Overbeek, J.T.G., and van Nes, K., 1948, *Theory of the Stability of Lyophobic Colloids: The Interaction of Sol Particles Having an Electric Double Layer*, Elsevier. ISBN: 978-0598458766.

Vogel, H.J., Weller, U., and Schlüter, S., 2010, Quantification of Soil Structure Based on Minkowski Functions, *Computers & Geosciences*, **36**(10), 1236–1245. DOI: 10.1016/j.caageo.2010.03.007.

Wenzel, R.N., 1936, Resistance of Solid Surfaces to Wetting by Water: *Industrial & Engineering Chemistry*, **28**(8), 988–994. DOI: 10.1021/ie50320a024.

White, M., Pierce, K., and Acharya, T., 2018, A Review of Wax-Formation/Mitigation Technologies in the Petroleum Industry, Paper SPE-189447, *SPE Production & Operations*, **33**(3), 476–485. DOI: 10.2118/189447-PA.

Zou, S., and Armstrong, R., 2019, Multiphase Flow Under Heterogeneous Wettability Conditions Studied by Special Core Analysis and Pore-Scale Imaging, Paper SPE-195577, *SPE Journal*, **24**(3), 1234–1247. DOI: 10.2118/195577-PA.

Zou, S., Armstrong, R. T., Arns, J.-Y., Arns, C.H., and Hussain, F., 2018, Experimental and Theoretical Evidence for Increased Ganglion Dynamics During Fractional Flow in Mixed-Wet Porous Media, *Water Resources Research*, **54**(5), 3277–3289. DOI: 10.1029/2017WR022433.

ABOUT THE AUTHORS

Maja Rücker is a Research Associate in the Chemical Engineering Department at Imperial College London working on the Shell Digital Rocks Program. Her research focus is on wettability and wettability-alteration effects on multiphase phase flow in porous media. She received her PhD in Petroleum Engineering in a joint project of the Rock & Fluid Physics team at Shell Global Solutions International B.V. and Imperial College London.

Willem-Bart Bartels has a background in earth sciences and hydrogeology. He holds a PhD degree from Utrecht University in collaboration with Shell Global Solutions International B.V. Currently, he works as a Flood Risk Consultant and Hydrogeologist for Lievense|WSP and as part-time professor at HAN University of Applied Sciences.

Tom Bultreys is a post-doctoral research fellow at Ghent University's Centre for X-ray Tomography. His research is focused on pore-scale physics of flow in porous media, and he is involved in methodological research on 3D and 4D X-ray imaging techniques that can be applied to this. Previously, he was a researcher at Imperial College London, where we worked on validating multiphase flow models. He obtained his PhD in physics and geology from Ghent University in 2016.

Marijn Boone is a product manager for micro-CT at TESCAN XRE NV in Belgium. His main research focus is on enabling and facilitating in-situ imaging and fast dynamic imaging using lab-based micro-CT systems, with a special interest in visualizing pore-scale processes in geological materials. He holds a PhD in Geology from Ghent University.

Kamaljit Singh is an Assistant Professor at Heriot-Watt University. Previously he was a research associate at Imperial College London, and postdoctoral researcher at the European Synchrotron Radiation Facility and Max Planck Institute for Dynamics and Self-Organization in collaboration with Saarland University. He received his PhD in Civil Engineering from the University of New South Wales at Australian Defence Force Academy. His research interests include three-dimensional imaging of flow in porous media with applications ranging from oil recovery, CO2 and hydrogen storage to biological systems, such as termite nests.

Gaetano Garfi is a PhD student in the Department of Earth Science and Engineering at Imperial College London. His research work focuses on wettability characterization and multiphase flow in porous media. He holds both a Bachelor's and a Master's degree in Energy Engineering from Politecnico di Milano, Italy.

Alessio Scanziani is a PhD candidate at Imperial College London, sponsored by the Abu Dhabi National Oil Company (ADNOC). His research mainly deals with the study of two- and three-phase flow in porous media, at the pore-scale, focusing on the flow dynamics and the effects of wettability alteration. Previously, he obtained a Master in Energy Engineering at Politecnico di Milano, Italy.

Catherine Spurin is a PhD researcher in the Department of Earth Science & Engineering at Imperial College London, funded by the President's PhD scholarship. Her research focus is on dynamics of multiphase flow in porous media using laboratory based micro-CT and fast synchrotron imaging.

Sherifat Yesufu-Rufai is a PhD student in the Department of Chemical Engineering at Imperial College London. She received her MSc from University College London and BEng from University of Benin, Nigeria. Her research focus is wettability alteration processes at the mineral-water interface studied with atomic-force microscopy (AFM).

Samuel Krevor is a Senior Lecturer in the Department of Earth Science & Engineering at Imperial College London. Previously he was a postdoctoral scholar at Stanford University. He received his PhD in Environmental Engineering from Columbia University. His research group investigates fundamental and applied aspects of subsurface fluid flow.

Martin J. Blunt is Shell Professor of Reservoir Engineering at Imperial College London. Previously he was a faculty member in the Department of Petroleum Engineering at Stanford University, and has also worked as a reservoir engineer for BP. He has a PhD in physics from Cambridge University. He performs theoretical, numerical and experimental research on multiphase flow in porous media with application to improved oil recovery and carbon dioxide storage.

Ove Bjorn Wilson is an experienced SCAL Senior Reservoir Engineer/ SCAL Subject Matter Expert with 25 years' experience in the oil industry. He has a PhD in Reservoir Engineering from NTNU in Norway. He has 10 years' experience working with field development studies (FDP) in Oman and Malaysia. He is currently supporting OUs and JVs from his position in Shell. In parallel with this, he is involved in research related to digital rock technology.

Hassan Mahani is currently Professor of Petroleum Engineering at the Department of Chemical and Petroleum Engineering of Sharif University of Technology. Before taking this position, he worked for about 12 years as principal investigator and research scientist at Shell Technology Centers in The Netherlands. Mahani's current research interests include low-salinity and engineered water EOR, wettability and rock-fluid interaction, pore-scale physics of multiphase flow and digital core analysis, and microscale experimentation. Mahani was recognized as an SPE Outstanding Technical Editor in 2015, 2016, 2017, 2018 and 2019, and a 2018 Top Reviewer by the American Chemical Society. He currently serves as associate editor for *SPE Reservoir Evaluation & Engineering* and *Journal of Petroleum Science and Engineering*. Mahani holds a PhD degree in petroleum engineering from Imperial College London and a master's degree in chemical engineering from Sharif University of Technology.

Veerle Cnudde received a PhD in Geology in 2005 from Ghent University (Belgium) where she became assistant professor in 2010. Since 2018 she is Full professor at the faculty of Science (Ghent University). She is team leader of PProGRess (www.pprogress.ugent.be), the Pore-scale Processes in Geomaterials Research group (Dept. of Geology, UGent) and is one of the coordinators of the Ghent University Expertise Centre for X-ray Tomography (UGCT). She specializes in nondestructive imaging of geomaterials and has a strong expertise in real-time imaging of processes in the pore space. Research projects which she has initiated are strongly linked to weathering and fluid-flow processes in porous sedimentary rocks, as well as conservation of building stones. In 2019, she obtained a dual professorship at the Environmental Hydrogeology group (Utrecht University, The Netherlands) in the field of "Porous media imaging techniques.

Paul F. Luckham is the Kodak Professor of interface science in the Department of Chemical Engineering at Imperial College London, He obtained his PhD in Physical Chemistry from the University of Bristol, undertook post-doctoral work in the Cavendish laboratory, Department of Physics, University of Cambridge and has been on the academic staff of Imperial College since 1983. He is an experimentalist working on many aspects of colloid and surface science, but principally in relating the nanoscopic properties of surfaces to their macroscopic behaviour.

Apostolos Georgiadis joined Shell in 2012, as Researcher in the Rock & Fluid Physics team. He obtained his PhD in 2011 and continued as Post-Doctoral Associate, both in Chemical Engineering under the Shell-Imperial College research program on Clean Fossil Fuels. His research has focused on capillary phenomena and phase behavior in the context of EOR and CCS processes, and more recently on pore-scale physics. His current involvement encompasses optical, Raman, and X-ray experimental development for further pore-scale characterization of both conventional and unconventional resources.

Steffen Berg is a principal science expert at Shell Global Solutions International B.V. in the Netherlands. His main research interests range from the fundamental aspects of multiphase flow in porous media to CO_2 sequestration, enhanced oil recovery, special core analysis and digital rock. He holds a masters degree in materials science from the University of the Saarland and a PhD in physics from the University of Mainz / Max Planck Institute for Polymer Research at Mainz, Germany. After a postdoc at Princeton University he joined Shell as a research scientist. He is currently also a visiting reader in the Earth Science & Engineering and Chemical Engineering departments at Imperial College London.